Published in final edited form as:
Eur J Neurosci. 2011 October ; 34(7): 1040–1052. doi:10.1111/j.1460-9568.2011.07836.x.

Roles of p53 and p27 ^{Kip1} in the regulation of neurogenesis in the murine adult subventricular zone

Sara Gil-Perotin[1,2], **Jeffery D. Haines**[3], **Jasbir Kaur**[3], **Mireya Marin-Husstege**[3], **Michael J. Spinetta**[4], **Kwi-Hye Kim**[3], **Maria Duran-Moreno**[1], **Timothy Schallert**[5], **Frederique Zindy**[6], **Martine F. Roussel**[6], **Jose M. Garcia-Verdugo**[7,1], and **Patrizia Casaccia**[3]

[1]Department of Comparative Neurobiology, CIBERNED, Valencia, Spain

[2]Intensive Care Medicine Unit, University Hospital La Fe, Valencia, Spain

[3]Department of Neuroscience Genetics and Genomics, Mount Sinai School of Medicine, New York, NY 10029, USA

[4]Department of Psychology, Seattle University, Seattle, WA, USA

[5]Department of Psychology, University of Texas, Austin, TX, USA

[6]Department of Tumor Cell Biology, St. Jude Children's Research Hospital, Memphis, TN, USA

[7]Department of Cell Morphology, Centro de Investigación Príncipe Felipe, Avda. V. A. Estellés, 46100 Burjassot Valencia, Spain

Abstract

The tumor suppressor protein p53 (*Trp53*) and the cell cycle inhibitor p27 ^{Kip1} (*Cdknb1*) have both been implicated in regulating proliferation of adult subventricular zone (aSVZ) cells. We previously reported that genetic ablation of *Trp53* (*Trp53* $^{-/-}$) or *Cdknb1* (*p27* $^{Kip1-/-}$) increased proliferation of cells in the aSVZ, but differentially affected the number of adult born neuroblasts. We therefore hypothesized that these molecules might play non-redundant roles. To test this hypothesis we generated mice lacking both genes (*Trp53* $^{-/-}$*;p27* $^{Kip1-/-}$) and analysed the consequences on aSVZ cells and adult neuroblasts. Proliferation and self-renewal of cultured aSVZ cells were increased in the double mutants compared with control, but the mice did not develop spontaneous brain tumors. In contrast, the number of adult-born neuroblasts in the double mutants was similar to wild-type animals and suggested a complementation of the *p27* $^{Kip1-/-}$ phenotype due to loss of *Trp53*. Cellular differences detected in the aSVZ correlated with cellular changes in the olfactory bulb and behavioral data on novel odor recognition. The exploration time for new odors was reduced in *p27* $^{Kip1-/-}$ mice, increased in *Trp53* $^{-/-}$ mice and normalized in the double *Trp53* $^{-/-}$*;p27* $^{Kip1-/-}$ mutants. At the molecular level, *Trp53* $^{-/-}$ *a*SVZ cells were characterized by higher levels of *NeuroD* and *Math3* and by the ability to generate neurons more readily. In contrast, *p27* $^{Kip1-/-}$ cells generated fewer neurons, due to enhanced proteasomal degradation of pro-neural transcription factors. Together, these results suggest that p27 ^{Kip1} and p53 function non-redundantly to modulate proliferation and self-renewal of aSVZ cells and antagonistically in regulating adult neurogenesis.

Correspondence: Dr Patrizia Casaccia and Dr Jose M. Garcia-Verdugo, [3]Department of Neuroscience Genetics and Genomics, and [7]Department of Cell Morphology, as above. patrizia.casaccia@mssm.edu and j.manuel.garcia@uv.es.

The authors have no competing interests to declare.

Keywords

cell cycle; neurogenesis; neurons; proliferation; stem cell; sub-ventricular zone

Introduction

Adult neural stem cells (aNSCs) continuously generate new neural cells and contribute to brain homeostasis, which is important for olfaction, plasticity and neural regeneration following brain damage. Due to the ability of aNSCs to proliferate and differentiate along different lineages, there have been a number of studies addressing their therapeutic potential after brain injury and their tumor-forming properties (Recht *et al.*, 2003; Picard-Riera *et al.*, 2004). Controlled expansion of multi-potential cells followed by differentiation along the desired cellular lineage represents a highly desirable outcome for therapeutic applications. Conversely, proliferative advantage coupled with impaired differentiation is associated with neoplastic transformation. There are two niches of aNSCs in the brain located in the subventricular zone (SVZ) and subgranular zone of the hippocampus (Doetsch *et al.*, 1999; Doetsch, 2003; Seri *et al.*, 2004). Three distinct cell subtypes have been classified in the SVZ, based on ultrastructural and molecular criteria (Doetsch *et al.*, 1997). Type B cells resemble astrocytes and are considered the bona fide aNSCs because they are capable of slow proliferation, multi-potentiality and self-renewal (Doetsch *et al.*, 1999). Type C cells are the transient-amplifying precursors that give rise to type A cells which differentiate into oligodendrocytes (Menn *et al.*, 2006) or the migratory neuroblasts. Type A cells born in the SVZ migrate along the rostral migratory stream (RMS), giving rise to olfactory bulb (OB) interneurons (Lois *et al.*, 1996) where they integrate within physiological neural networks and mediate memory of new odors and exploratory behavior of novel odors (Magavi *et al.*, 2005).

Two cell cycle regulators that control cell cycle exit and cell fate decisions of aNSCs are p27 ^{Kip1} and p53 (Doetsch *et al.*, 2002; Gil-Perotin *et al.*, 2006). p27 ^{Kip1} is a cyclin-dependent kinase inhibitor, encoded by the *Cdknb1* gene and initiates exit from the cell cycle. p53 is a sequence-specific DNA-binding transcription factor encoded by the gene *Trp53*, and induces apoptosis or cell cycle arrest in response to genotoxic stress, thus blocking the transmission of DNA mutations to progeny cells (Sherr & Roberts, 1995). We have previously shown that mice lacking the N-terminal portion of p27 ^{Kip1}, due to deletion of the first exon of *Cdknb1*, have more transit-amplifying progenitors and fewer neuroblasts compared with wild-type littermates (Doetsch *et al.*, 2002). We also showed that loss of *Trp53* provided a proliferative advantage to the adult SVZ (aSVZ) populations and, in association with their rapid differentiation, resulted in an increased number of new neurons and oligodendrocytes (Gil-Perotin *et al.*, 2006; Li *et al.*, 2008). As *CDKNB1* and *TP53* are two critical regulators of the cell cycle, they are expressed in the SVZ and their mutations are often detected in adult human tumors, we reasoned that crossing *Trp53* $^{-/-}$ and *p27* $^{Kip1-/-}$ mice might lead to a transformed phenotype. Here we report the phenotype of mice lacking both genes (i.e. *Trp53* $^{-/-}$*;p27* $^{Kip1-/-}$ compound mutants), and suggest a non-redundant role of these two molecules on the proliferation of aSVZ cells and an antagonistic effect on the generation of adult neuroblasts.

Materials and methods

Animals

All animal experiments were performed in accordance with guidelines approved by the Mount Sinai School of Medicine Animal Care Committee. All the experiments were performed in 8- to 12-week-old mice obtained by crossing B6.129S2-*Trp53* ^{tm1Tyj}/J

heterozygous (i.e. *Trp53*$^{+/-}$) from Jackson Laboratories and *p27* ^{Kip1} breeding pairs (Fero *et al.*, 1996). Mouse genotypes were confirmed by tail-clipping and PCR using primers 5′-ACAGCGTGGTGGTACCTTAT-3′ (ImRo36), 5′-TATACTCAGAGCCGGCCT-3′ (ImRo37) and 5′-TCC TCGTGCTTTACGGTATC-3′ (neo), yielding a fragment of 375 bp in *Trp53*$^{+/+}$ and 525 bp in *Trp53*$^{-/-}$ mice, and 5′-TGGAACCCTGTG-CCATCTCTAT-3′ (MgK3), 5′-CCTTCTATGGCCTTCTTGACG-3′ (Neo-1) and 5′-GAGCAGACGCCCAAGAAG-3′ (MgK5) yielding a fragment of 500 bp in *p27* $^{Kip1+/+}$ and 1000 bp in *p27* $^{Kip1-/-}$ mice.

SVZ dissection

The SVZ was dissected from coronal slices of 2 mm thickness, anteriorly defined by the presence of the anterior commissure and posteriorly defined by the rostral opening of the third ventricle. A strip of tissue (100 μm wide; 2–4 mm long) was cut along the lateral wall of the lateral ventricle from the region below the corpus callosum to the ventral tip of the lateral ventricle, as previously described (Lois & Alvarez-Buylla, 1993).

Immunohistochemistry and immunocytochemistry

For immunocytochemical and immunohistochemical procedures, a detailed description of the primary antibodies and references related to their specificity is presented in Table 1. Additional controls for immunocytochemistry included incubation with only the secondary antibody and, in some cases, pre-incubation with blocking peptide. Immunoreactive cells were analysed using a fluorescence microscope (Leica, Heerbrugg, Switzerland) and images were captured using a Hamamatsu CCD camera interfaced with a computer and processed as previously described (He *et al.*, 2007). Confocal images were captured with a Zeiss 710 microscope.

TUNEL *in vivo*

Trp53$^{+/+}$ and *Trp53*$^{-/-}$ mice were perfused with 4% paraformaldehyde. Brains were removed, cryopreserved in 30% sucrose and sectioned. Sections were treated with 100% ethanol/acetic acid (2:1) for 10 min at −20 °C, washed three times in PBS and processed with Apoptag® Plus Fluorescein In Situ Detection kit (Chemicon, Temecula, CA, USA) according to the manufacturer's instructions.

Immunoprecipitation and western blotting

Whole-cell lysates were prepared from the OB and SVZ of *p27* $^{Kip1-/-}$ and *Trp53*$^{-/-}$ mice in lysis buffer (50 mM HEPES, pH 7.4, 150 mM NaCl, 1% NP-40, 1.0 mM EDTA, 10% glycerol, 1 mM dithiothreitol, 1 mM PMSF). The SVZ was dissected as described above. The brain areas were homogenized and debris was centrifuged. Between 1 and 2 mg of post-nuclear supernatant was pre-cleared with 20 μL of protein G sepharose (Santa Cruz Biotechnology, Santa Cruz, CA, USA) and normal rabbit IgG for 1 h at 4 °C. Two micrograms of mouse anti-Ngn2 (for immunoprecipitation we used antibody N6286 from Sigma-Aldrich, St Louis, MO, USA) was added to the pre-cleared supernatants and rocked overnight at 4 °C. The immune complexes were captured using 20 μL of protein G sepharose for 1 h and washed four times with lysis buffer. Pelleted complexes were boiled in Laemmli sample buffer, electrophoresed and immunoblotted with anti-p27 ^{Kip1} 1: 200 (sc-4091, Santa Cruz Biotech), anti-Ngn2 1: 200 (kindly provided by Dr Y. Ma, Harvard University, Boston, MA, USA) or rabbit anti-p53 1: 1000 (Novacastra, Newcastle, UK) antibodies. The experiment was independently replicated using a rabbit polyclonal p27^{Kip1} antibody (Santa Cruz, sc-528) for immunoprecipitation followed by western blotting with rabbit Ngn2 antibody (Millipore, AB5682). The specificity of the p27^{Kip1} antibody was

validated using purified recombinant p27 protein (Santa Cruz, sc-4091) and brain lysates from knockout mice. Three different anti-Ngn2 antibodies were used to verify specificity.

Electron microscopy

For the quantification of individual cell types, ultrathin (60 nm) sections were cut with a diamond knife, stained with lead citrate and examined under a JEOL 1010 transmission electron microscope (Tokyo, Japan). The number of profiles corresponding to each different cell type was counted along the ventricular wall of the anterior horn of the SVZ following the criteria described by Doetsch *et al.* (1997). The dorsolateral corner of the SVZ was excluded from the analysis, because the high density of cells did not allow an accurate quantification. Graphical exploration of our data indicated that we could safely assume homogeneity of variance and normal distribution. Thus, we used a Student's *t*-test to analyse the differences in cell number in the SVZ. All reported probabilities were two-tailed. Significance level for the rejection of the null hypothesis was set at $P = 0.05$.

Thymidine labeling and autoradiography

Mice were injected with 50 μL of 6.7 mCi tritiated thymidine (^{3}[H]-Thy, GE Healthcare, Piscataway, NJ, USA) as previously described (Doetsch *et al.*, 2002). One hour after injection, mice were perfused with 0.9% saline followed by Karnovsky's fixative (2% paraformaldehyde and 2.5% glutaraldehyde). Heads were removed and post-fixed in the same fixative overnight, and the brains were dissected, washed in 0.1 M phosphate buffer and cut into 200-μm vibratome sections. Sections were post-fixed in 2% osmium tetroxide and embedded in araldite (Durcupan, Fluka, St Louis, MO, USA). Semithin sections (1.5 μm) were processed for autoradiography (Doetsch *et al.*, 2002). Ultrastructural identification of ^{3}[H]-Thy-positive cells was conducted in five sections (one every 7.5 μm), of the same region of the SVZ which lies immediately posterior to the optic chiasm. Fifty ^{3}[H]-Thy+ cells per genotype were identified (200 cells in total). Average counts were calculated and extrapolated per mm^2.

Neurosphere cultures

Cells were collected from the SVZ dissected from wild-type, *p27* $^{Kip1-/-}$, *Trp53*$^{-/-}$ and *Trp53*$^{-/-}$;*p27* $^{Kip1-/-}$ mice in Petri dishes containing Pipes buffer (20 mm PIPES, 25 mM glucose, 120 mM NaCl, 0.5 mM KCl, pH 7.4). After digestion with papain, cells were dissociated and resuspended in Neurobasal medium (supplemented with B27, 2 mM L-glutamine, Antibiotic/Antimycotic), all from Gibco BRL (Invitrogen, Carlsbad, CA, USA), and 2 μg/mL heparin (Sigma). Equal numbers of cells (10 000 cells/cm^2 for experiments at high density, 1000 cells/cm^2 for experiments at low density) were plated and kept in medium containing 20 ng/mL recombinant mouse receptor-grade epidermal growth factor (Millipore) and 10 ng/mL basic fibroblast growth factor (Peprotech, Rocky Hill, NJ, USA). The number of primary neurospheres was counted after 7 days. For the differentiation studies, the primary neurospheres were mechanically dissociated and the cells were then plated in poly-ornithine-coated chamber slides without mitogens in the presence (or absence) of 1% fetal bovine serum (FBS) and B27 supplement. Self-renewal was calculated by dissociating individual secondary and tertiary neurospheres into single-cell suspensions and transferring them into individual wells of a 96-well plate and counting the total number of neurospheres generated after 5 days.

Treatment of SVZ cultured cells with MG132

The proteasome inhibitor MG132 was purchased from Calbiochem and dissolved to 100 mM in ethanol and diluted to working concentrations of 0.5 and 5.0 μM. These concentrations were chosen on the basis of a defined IC_{50} of 100 nM and previous reports

on the toxicity of the molecule in neuroblasts at concentrations of 10 μM and higher (Sun *et al.*, 2006). Treatment with the inhibitor was carried out for 6 h as previously reported (Andela & Rosier, 2004; Rane *et al.*, 2004). Cultured aSVZ cells were allowed to form neurospheres for 7 days and then dissociated and re-plated on poly-ornithine-coated chamber slides and kept in differentiation conditions for 1 or 3 days. For the MG132 treatment, 5.0 μM was added to the medium on day 1 or day 3 of differentiation for 6 h and the cells were then fixed and stained. The experiment was performed in duplicate in three separate experiments.

RNA extraction and quantitative real-time qPCR

Freshly dissected SVZ regions (n = 3 for each genotype) were homogenized in Trizol® reagent. RNA was isolated using the RNeasy Mini kit (Qiagen, Hilden, Germany). Then, 1.5 μg of total RNA was reverse-transcribed and amplified using SuperScript® and random hexamers (Invitrogen). The linear phase of logarithmic amplification was used for quantification and cycle number was compared between triplicate samples. SYBR green was used on an ABI prism machine according to the manufacturer's instructions. The primers used were as follows: *Math3* forward, 5′-ATTCAGGGCTCGAAGAGTCA-3′; *Math3* reverse, 5′-TTCCTTTGCCAGTCGAAGAGT-3′; *NeuroD* forward, 5′-GCGAGATCCCCATAGACAACAT-3′; *NeuroD* reverse, 5′-CATTAAGCTGGGCACTCATGAC-3′.

Odor recognition test

The social odor recognition experiments were performed as previously described (Spinetta *et al.*, 2008; O'Dell *et al.*, 2010; Monaghan *et al.*, 2010). During learning/habituation, each mouse was presented in the home cage with four small wooden spheres (2.5 cm diameter), three of which were highly familiar (i.e. had been recently taken from that same animal's home cage and therefore were laden only with self-odors) and one of which was taken from the cage of a different mouse (novel odor donor). Three 1-min trials were conducted for thorough habituation to novel odors. The odor recognition test was carried out 24 h later, at which time the mouse was presented with a novel odor-laden sphere (which it had explored for the first time on the day before and designated as 'habituated odor') together with a sphere laden with a brand new social odor taken from a new mouse's cage (designated 'novel odor') and two highly familiar spheres again from the target mouse's home cage. Normal mice have intact overnight memory for the habituated odor and thus spend less time exploring it compared with the novel odor (Spinetta *et al.*, 2008; modified from Ma *et al.*, 2008). Memory impairment would lead to statistically equal time exploring the recently habituated and the novel odor sphere. No interest in any particular stimulus would be represented as 25% on each odor sphere, and (using time rather than percentage time) no exploration at all would indicate non-specific deficits (this did not occur in this study).

Long-term BrdU incorporation and olfactory bulb cell counts

Mice received a total of five BrdU injections (dose 50 mg/kg body weight) every 2 h for a total of 10 h. Two weeks later they were perfused with saline, followed by fixation in 4% paraformaldehyde. After cryopreservation, the OBs were sectioned and processed for double immunofluorescence, using antibodies specific for BrdU (anti-rat ab6326; Abcam, Cambridge, MA, USA) and for NeuN (anti-mouse MAB377; Millipore Inc., Billerica, MA, USA). The optical dissector method was performed to count cells and the results are expressed as number of cells per volume unit (mm^3).

Statistical analysis

Graphs were constructed and data analysed using GraphPad Prism 5.0 software (La Jolla, CA, USA). After assessing the homogeneity of variance with the Levene's test and graphically, one-way analysis of variance (ANOVA) followed by a Dunnett's multiple-comparison test were used to determine statistical differences following quantification of cell types by transmission electron microscopy and mitoses, for amplification, size and self-renewal rates of neurospheres. The Mann–Whitney *U*-test was used for *in vitro* quantifications of glial fibrillary acidic protein (GFAP) and TuJ1. Independent two-tailed *t*-tests were used to determine statistical differences in ^{3}[H]-Thy incorporation, BrdU-NeuN expression *in vivo* in the OB, and to analyse differences in *NeuroD* and *Math3* levels by qPCR and for the proteasome inhibitor experiments. The odor recognition data were analysed using a *t*-test on the difference scores by calculating the difference of mean score for a novel odor relative to the habituated odor, compared with $Trp53^{+/+};p27^{Kip1+/+}$ mice. All results were considered statistically significant at $P < 0.05$.

Results

The goal of our study was to determine the functional consequences of *Trp53* and $p27^{Kip1}$ loss in the adult SVZ. We had previously characterized the phenotype of mice lacking the first exon of *Cdknb1* (Doetsch *et al.*, 2002) or mice lacking *Trp53* (Gil-Perotin *et al.*, 2006). In the present study we crossed mice with a complete deletion of *Cdknb1* ($p27^{Kip1-/-}$ mice) with those lacking *Trp53* ($Trp53^{-/-}$ mice) to generate the $Trp53^{-/-};p27^{Kip1-/-}$ double mutants. These mice were phenotypically normal. They did not display any overt neurological signs nor did they develop brain tumors. To better characterize the effect of deletion of both *Cdknb1* and *Trp53* on aNSCs, we analysed the SVZ in 9- to 12-week-old $Trp53^{-/-};p27^{Kip1-/-}$ mice and compared it with single mutants and wild-type littermates.

The cell cycle regulators p53 and $p27^{Kip1}$ differentially regulate the number of aSVZ cells

Toluidine blue staining of semithin sections revealed hyperplastic changes in both the $Trp53^{-/-}$ and the $Trp53^{-/-};p27^{Kip1-/-}$ double mutants (Fig. 1B–D), although none of the mice developed spontaneous tumors. To determine the total number of cells in each aSVZ subpopulation, we performed electron microscopic analysis of tissue sections of the adult SVZ from the different genotypes of mice (Fig. 1E and F). The numbers of A, B, C and E cells was determined based on their distinct morphologies, as we have previously described (Doetsch *et al.*, 2002). Briefly, A cells (neuroblasts) were identified by their elongated morphology, scant dark cytoplasm, abundance of free ribosomes and microtubules oriented along the longitudinal axis of the cells. Type B cells (SVZ astrocytes) were characterized by multiple processes that intercalate amongst other cells, thick bundles of intermediate filaments, and glycogen granules and dense bodies in the cytoplasm and gap junctions. Type C cells (transit-amplifying progenitors) were defined as more electron-dense than type B cells and more electron translucent than A cells (Doetsch *et al.*, 1997). E cells were ependymal cells lining the lumen of the ventricles. The number of type A neuroblasts in $Trp53^{-/-}$ mice (mean ± SD, 118.9 ± 7.6 cells/mm^2) was greater than in wild-type, but was lower in $p27^{Kip1-/-}$ mice lacking the entire *Cdknb1* gene (26.6 ± 4.88 cells/mm^2) than wild-type littermates (67.6 ± 0.42 cells/mm^2; ANOVA: d.f. = 3; d.f. = 9, $F = 52{,}005$, $P = 0.000$; $n_C = 3$, $n_{p53} = 3$, $n_{p27} = 5$, $n_{p27p53} = 2$). This was consistent with our previous findings in mice lacking only the N-terminal portion of the p27 ^{Kip1} molecule (Doetsch *et al.*, 2002). The $Trp53^{-/-};p27^{Kip1-/-}$ mice had similar numbers of A neuroblasts (67.8 ± 8.1 cells/mm^2) to wild-type, suggesting a genetic complementation of the *Cdknb1* deletion by loss of *Trp53* in regulating the generation of adult neuroblasts from the aSVZ. A significantly greater number of B cells detected in the aSVZ of $Trp53^{-/-}$ mice (97.4 ± 6.78 cells/mm^2; ANOVA: d.f. = 3; d.f. = 9, $F = 3{,}96$, $P = 0.047$) compared with wild-type mice (78.6 ± 0.02 cells/

mm^2). The number of C cells was not statistically higher in *Trp53*$^{-/-}$ mice (ANOVA: d.f. = 3; d.f. = 9, F = 1,779, P = 0.221) than wild-type (30.8 ± 2.11 cells/mm^2), but was increased in *p27* $^{Kip1-/-}$ mice (41.9 ± 3.78 cells/mm^2, $P < 0.05$) and to a higher degree in the *Trp53*$^{-/-}$*;p27* $^{Kip1-/-}$ double mutants (43.7 ± 0.1 cells/mm^2, P = 0.001). Together these data suggest that p27 ^{Kip1} and p53 differentially modulate the number of aSVZ cells in distinct subpopulations and that deletion of both genes results in the expansion of the stem cell and transit-amplifying compartments.

Roles for p53 and p27 ^{Kip1} in the regulation of proliferation and clonal expansion of aSVZ cells

To define the consequences of ablating either one or both genes on proliferation of aSVZ cells, we used pulse incorporation of ^{3}[H]-Thy followed by autoradiography and quantified the total number of ^{3}[H]-Thy+ aSVZ cells in animals of distinct genotypes (Fig. 2A). Although we detected a higher number of ^{3}[H]-Thy+ aSVZ cells in *Trp53*$^{-/-}$, *p27* $^{Kip1-/-}$ and *Trp53*$^{-/-}$*;p27* $^{Kip1-/-}$ mice compared with controls, only the *Trp53*$^{-/-}$ mice showed statistically significant differences (t-test: d.f. = 3, t =)4,607, P = 0.019). To further characterize the proliferative capacity of the aSVZ cells, we counted the number of mitotic figures by electron microscopy (Fig. 2B). The number of mitoses in *Trp53*$^{-/-}$ mice (1.5 ± 0.22 mitoses/mm^2) was similar to that detected in *p27* $^{Kip1-/-}$ mice (1.56 ± 0.31 mitoses/mm^2) and was almost two-fold higher than the number of mitoses detected in wild-type mice (0.84 ± 0.11 mitoses/mm^2). Interestingly, in *Trp53*$^{-/-}$*;p27* $^{Kip1-/-}$ mice the number of mitoses was even higher, but not additive (1.82 ± 0.02 mitoses/mm^2) being in all cases significantly higher than in wild-type littermates (ANOVA: d.f. = 3; d.f. = 8, F = 14,365, P = 0.001; n_C = 3, n_{p53} = 3, n_{p27} = 3, n_{p53p27} = 3). Therefore, deletion of two critical cell cycle regulators did not result in additive or synergistic effects on proliferation and suggested that p53 and p27 ^{Kip1} converge on a common regulatory pathway of proliferation.

Population dynamics in the SVZ is regulated by an equilibrium between self-renewal, proliferation, survival and differentiation. We therefore systematically analysed whether lack of *Trp53* or *Cdknb1* affected each of these properties. Self-renewal was measured by the ability of aSVZ cells to form neurospheres that can be serially passaged (Fig. 2C). At high plating density (10 000 cells per well) the *Trp53*$^{-/-}$ aSVZ displayed a significantly higher number of neurospheres compared with wild-type (t-test: d.f. = 6, t = −3,45, P = 0.018), while the increased number of neurospheres detected in cultures from mice lacking *p27* $^{Kip1-/-}$ or both *Trp53*$^{-/-}$*;p27* $^{Kip1-/-}$ was not statistically significant (Fig. 2D). Because self-renewal encompasses the property of clonogenic expansion, which is retained after serial passages, we tested the ability of individual spheres to form neurospheres after dissociation into a single cell suspension and re-plating in 96-well plates (Fig. 3). In this case we detected a clear difference between cells from the double knockouts and those from single mutants in secondary (Fig. 3B) and tertiary (Fig. 3D) passages. It is worth mentioning that neurospheres from mice with distinct genotypes were characterized by differences in size that became more evident with serial passages (Fig. 3). While neurospheres from *Trp53*$^{-/-}$, *p27* $^{Kip1-/-}$ or from *Trp53*$^{-/-}$*;p27* $^{Kip1-/-}$ mice were larger than wild-type during the first passage (Figs 2C, and 3A, C and E), at the second passage only the neurospheres derived from *Trp53*$^{-/-}$*;p27* $^{Kip1-/-}$ aSVZ cells (average size = 442.89 ± 29.58 μm, P = 0.001) were twice as large as those derived from wild-type cells (average size = 200.69 ± 32.03 μm) and this difference persisted after repeated passages of the cells (t-test: d.f. = 12, t = 5.605, P = 0.00011). These results are consistent with the results of the cell counts, supporting an increase of both stem cell and transit-amplifying progenitors only in the double mutants.

Distinct roles for p53 and p27 ^{Kip1} in the generation of adult neuroblasts from aSVZ cells

To further define the role of these molecules in neurogenesis, we dissociated aSVZ cells from mice of the four distinct genotypes, plated them on laminin substrate and cultured them in chemically defined medium, in the absence of mitogens for 7–10 days to allow differentiation (Fig. 4). After culturing these cells *in vitro* in differentiating conditions, we noted significant differences in the ability to generate neuroblasts (Fig. 4A). While wild-type aSVZ cells grown in these conditions typically generated 19 ± 1% TuJ1+ neuroblasts, we detected a statistically significant increase of neuroblast generation in cells lacking *Trp53* (62 ± 4.1%; Mann–Whitney *U*-test: $Z = -2{,}309$, $P = 0.029$, $n_c = 4$; $n_{p53} = 4$) and a statistically significant decrease in cells from mice lacking *p27 ^{Kip1}* (5 ± 0.97%; Mann–Whitney *U*-test: $Z = -2{,}309$, $P = 0.029$, $n_c = 4$; $n_{p27} = 4$) (Fig. 4B). Notably, the differentiation of *Trp53 $^{-/-}$; p27 $^{Kip1\,-/-}$* cells led to a number of neuroblasts (20 ± 3.1%; Mann–Whitney *U*-test: $Z = -0{,}577$, $P = 0.686$, $n_c = 4$; $n_{p53p27} = 4$) equivalent to that of wild-type, thereby suggesting that the concomitant loss of *p27 ^{Kip1}* with *Trp53* prevents the increase in neurogenesis. The number of GFAP+ glial cells, in contrast, was not statistically different among aSVZ cells from distinct genotypes (Fig. 4C and D), although the morphology of astrocytes generated from *Trp53 $^{-/-}$;p27 $^{Kip1\,-/-}$* cells was characterized by thin and long cytoplasmic processes that were not observed in any other genotype (Fig. 4C). These data suggested that p53 and p27^{Kip1} play distinct and opposing roles in neurogenesis.

To confirm the effect of these cell cycle regulators on newly generated adult neuroblasts in the SVZ, we performed staining of tissue sections from mice of the four different genotypes, with an antibody specific for the neuronal marker doublecortin (Fig. 5). In agreement with the *in vitro* TuJ1 data and the quantitative electron microscopic determination, we detected an increased area of double-cortin immunoreactivity in *Trp53 $^{-/-}$* and a decreased area in *p27 $^{Kip1\,-/-}$* compared with wild-type. The pattern of immunoreactivity in *Trp53 $^{-/-}$;p27 $^{Kip1\,-/-}$* was similar to wild-type (Fig. 5A and B) and similar results were also obtained in immunohistochemical experiments using antibodies specific for TuJ1. Thus, the immunohistochemical data were consistent with the cell counts by electron microscopy and with the cell culture experiments.

p27 $^{Kip1-/-}$ mice exhibit defects in novel odor recognition that are rescued by deletion of Trp53

It has been previously shown that adult-born neuroblasts in the SVZ migrate to the OB, where they integrate in cellular networks responsible for the familiarization to novel odors (Magavi *et al.*, 2005). As *Trp53 $^{-/-}$*, *p27 $^{Kip1\,-/-}$* and *Trp53 $^{-/-}$;p27 $^{Kip1\,-/-}$* mice showed differences in the number of adult-generated neuroblasts, we asked whether differences in adult neurogenesis in *Trp53 $^{-/-}$* or *p27 $^{Kip1\,-/-}$* mice would affect the number of cells in the OB and modulate odor-seeking behavior or odor recognition. To determine whether the increased neurogenesis detected at the level of the anterior SVZ resulted in the generation of new neurons in the OB and potentially modulate olfactory behavior, we performed a long-term BrdU experiment. Briefly, mice of the four different genotypes were injected with BrdU (five doses within 10 h) and then the OBs were analysed 2 weeks later. The number of BrdU/NeuN+ cells was quantified using the optical dissector method and revealed a similar trend as the reported cell counts in the SVZ, although it did not reach statistical significance (Fig. 6A and B). The mean number of BrdU/NeuN+ cells in the *p27 $^{Kip1\,-/-}$* mice was 22.54 ± 5.68 cells/mm^3, lower than the value for wild-type mice (29.59 ± 8.45 cells/mm^3). For *Trp53 $^{-/-}$* mice the mean of 50.41 ± 4.84 cells/mm^3 was greater than that of the wild-type and the double mutant *Trp53 $^{-/-}$;p27 $^{Kip1\,-/-}$* had intermediate numbers (37.25 ± 7.39 cells/mm^3). To translate these cellular data in behavioral terms, we conducted experiments on odor recognition and the results were analysed by investigators blind to the genotype. We detected overnight memory impairment in *p27 $^{Kip1\,-/-}$* mice that failed to show a relative

decrease in the percentage of time exploring a previously habituated social odor (0.46 ± 0.07% exploration time; *t*-test: d.f. = 9, $t = -2{,}99$, $P = 0.021$) and increased amount of time exploring a novel odor (0.29 ± 0.09% exploration time; *t*-test: d.f. = 10, $t = 2{,}602$, $P = 0.033$) relative to wild-type siblings (habituated odor: 0.20 ± 0.05% exploration time; novel odor: 0.56 ± 0.05% exploration time) (Fig. 6D). Meanwhile, *Trp53*$^{-/-}$ mice showed normal memory, and even a trend towards a relative increase in novel odor exploration, relative to wild-type animals, which did not reach significance (Fig. 6D). Importantly, in *p27*$^{Kip1-/-}$ mice the exploration time towards habituated and novel odors was increased relative to that of highly familiar home-cage odor spheres (used as controls for non-specific odors). Therefore, we conclude that memory impairment rather than a non-specific impairment of odor exploration was the likely cause of the observed behavior. Thus, there were no detectable differences between time spent exploring a novel odor and a habituated odor, consistent with memory impairment. However, there was no statistically significant difference in the *Trp53*$^{-/-}$*;p27* $^{Kip1-/-}$ mice compared with normal littermates (Fig. 6D), suggesting that p53 and p27 ^{Kip1} have at least partially opposing roles in the regulation of OB interneuron formation, ultimately affecting novel odor-seeking behavior.

Trp53 loss-of-function results in precocious transcriptional activation of neurogenic genes while p27 ^{Kip1} stabilizes Ngn2 and increases its protein levels to promote neurogenesis

Because *Trp53* deletion rescued the neurogenic deficit of *p27* $^{Kip1-/-}$ mice we investigated whether this effect could be simply explained in terms of increased survival or also due to additional effects on the transcriptional regulation of neurogenesis. We previously reported that *p27* $^{Kip1-/-}$ mice have increased apoptosis, while no significant difference in physiological apoptosis was detected between wild-type and *Trp53*$^{-/-}$ mice (Gil-Perotin *et al.*, 2006). In agreement with the hypothesis that ablation of *Trp53* compensated for the increased death in the *p27* $^{Kip1-/-}$ mutants (16 ± 0.1), the number of TUNEL-positive cells per surface area in the SVZ of *Trp53*$^{-/-}$*;p27* $^{Kip1-/-}$ mice (1.4 ± 0.2) was similar to that measured in wild-type animals (data not shown). These results were also consistent with the similar number of pyknotic nuclei detected in wild-type, *Trp53*$^{-/-}$ and *Trp53*$^{-/-}$*;p27* $^{Kip1-/-}$ by electron microscopy (data not shown).

We reasoned that a positive effect of *Trp53* deletion on adult SVZ neurogenesis could be best evaluated by precocious detection of proneural genes in cultured cells. For this reason, *Trp53*$^{-/-}$ SVZ cells were maintained in differentiating conditions for 1, 3 and 7 days and then harvested for immunocytochemistry and mRNA isolation. TuJ1 staining revealed the presence of several TuJ1+ cells as early as after 3 days in differentiating conditions (Fig. 7A). The appearance of these neuroblast markers was accompanied by the detection of higher transcript levels of the proneural genes at 3 days *in vitro*, including *NeuroD* and *Math3*, in *Trp53*$^{-/-}$ (*NeuroD*: 0.38 ± 0.01; *t*-test: d.f. = 4; $t = -5.613$; $P = 0.019$; $n_{p53} = 3$; *Math3*: 0.72 ± 0.01; *t*-test: d.f. 4; $t = -34.7$; $P < 0.001$) compared with wild-type (*NeuroD*: 0.17 ± 0.03; *Math3*: 0.15 ± 0.013) (Fig. 7B and C). These data suggested that p53 activity negatively regulated the expression of neurogenic basic Helix-Loop_helix transcription factors.

It was previously reported that p27 ^{Kip1} regulates the stability of the neurogenic transcription factor Ngn2, by direct binding and protection from proteolytic degradation (Nguyen *et al.*, 2006). Because *p27* $^{Kip1-/-}$ mice were characterized by lower numbers of adult-generated neuroblasts in the SVZ, we investigated whether a similar event could occur in aSVZ cells. Ngn2 expression was validated by real-time PCR, chromatin immunoprecipitation using RNApol II antibodies (data not shown) and western blot analysis (Fig. 7D). Immunoprecipitation of protein extracts from the SVZ and OB of wild-type animals using antibodies specific for the N terminus of Ngn2, followed by western blot analysis with antibodies specific for p27 ^{Kip1} or for p53, revealed the presence of a protein complex

between Ngn2 and p27^{Kip1}, which was confirmed also by performing reverse immunoprecipitation with p27 ^{Kip1} antibodies, followed by western blot analysis with antibodies specific for the N-terminal domain of murine Ngn2 (Fig. 7D). When the experiment was repeated with antibodies specific for Mash1 and p27 ^{Kip1}, no complex was detected (data not shown). These data suggested the possibility that SVZ cells lacking *p27 ^{Kip1}* might have impaired ability to form neuroblasts due to proteasomal degradation of Ngn2. To test this hypothesis, we cultured SVZ cells from *p27 $^{Kip1-/-}$* and wild-type mice in differentiation conditions for 1 or 3 days in the presence of the proteasome inhibitor MG132 and assessed the number of TuJ1+ neuroblasts. In the presence of MG132, cells lacking *p27 ^{Kip1}* generated the same number of neuroblasts as wild-type cells after 3 days *in vitro* (control wild-type: 0.4 ± 0.02; *p27 $^{Kip1-/-}$*: 0.1 ± 0.08; *t*-test: d.f. = 4; $t = 3{,}18$; $P = 0.048$; $n_{wt} = 3$; $n_{p27} = 3$; MG132 wild-type: 0.38 ± 0.1; *p27 $^{Kip1-/-}$*: 0.45 ± 0.08; *t*-test: d.f. 4; $t = -0.551$; $P = 0.612$; $n_{wt} = 3$; $n_{p27} = 3$) (Fig. 7E). Thus, the proteasome inhibitor MG132 restored the number of TuJ1-positive neurons in *p27 $^{Kip1-/-}$* cultures, suggesting that, in physiological conditions in aSVZ cells, p27 ^{Kip1} might serve a protective role towards Ngn2 protein stability and favor neurogenesis.

Discussion

Role of p53 and p27 ^{Kip1} in modulating the properties of SVZ cells

This study addresses the role of the cell cycle regulators p27 ^{Kip1} and p53 in modulating proliferation and differentiation of adult neural stem cells residing in the SVZ (Doetsch *et al.*, 2002; Gil-Perotin *et al.*, 2006). The rationale for such a study is based on the previous detection of mutations of the genes coding for p53 (*TRP53*) and p27 ^{Kip1} (*CDKNB1*) in human cancers (van Meyel *et al.*, 1994; Rasheed *et al.*, 1994; Park *et al.*, 2004; Temme *et al.*, 2010) and their expression pattern in the SVZ, a germinal region of the adult brain, where adult neural stem cells reside (Morrison *et al.*, 1997; Doetsch *et al.*, 1999; Johansson *et al.*, 1999; Mirzadeh *et al.*, 2008). aSVZ cells are pluripotent cells with the ability to differentiate into neurons, astrocytes and oligodendrocytes. These cells are characterized by the clonogenic property of self-renewal and by the ability to grow in suspension, as aggregates of undifferentiated cells called neurospheres (Reynolds *et al.*, 1992). Because of these properties, it has been proposed that these cells could be the cell-of-origin of brain tumors in the adult population. We have previously reported that prenatal exposure to *N*-ethyl-*N*-nitrosourea was also responsible for the induction of glioblastoma multiformes in mice lacking *Trp53* (Gil-Perotin *et al.*, 2006), and hypothesized that mutation or loss of the two critical cell cycle regulators p53 and p27 ^{Kip1} could provide a selective proliferative advantage to the SVZ cell population and possibly also affect the ability of these cells to differentiate, thereby rendering them more susceptible to cancer formation.

In this study we show that genetic deletion of both *Trp53* (coding for p53) and *Cdknb1* (coding for p27 ^{Kip1}) did not result in increased tumorigenic potential of SVZ cells, but provided a better understanding of the regulation of the population dynamics in terms of self-renewal and neurogenesis.

Role of p53 and p27 ^{Kip1} in modulating adult neurogenesis

An interesting observation, however, was the detection of a genetic complementation on neurogenesis. We had previously reported that mice lacking the first exon of *Cdknb1* (Kiyokawa & Koff, 1998) and therefore characterized by loss of the N-terminal portion of p27 ^{Kip1} were characterized by a defective number of type A SVZ cells or neuroblasts (Doetsch *et al.*, 2002). Possible reasons for decreased numbers of neuroblasts included: decreased generation, increased cell death, dispersal, or a combination of these three events. In our previous study we reported increased apoptosis in the SVZ of these mice (Doetsch *et*

al., 2002), although we could not exclude the other two possibilities. Because mice retained the C-terminal domain of p27 ^{Kip1} and this region of the molecule is capable of interacting with the actin cytoskeleton (McAllister *et al.*, 2003), we reasoned that dispersal could at least partly explain why we detected fewer neuroblasts in the SVZ. For this reason, in this study we entirely focused our analysis on *p27* $^{Kip1-/-}$ mice with a complete deletion of the gene (Mullen *et al.*, 1992). The fact that also mice lacking *p27* ^{Kip1} showed decreased neuroblast numbers strongly supported the idea that p27 ^{Kip1} modulated adult neurogenesis. We have also previously reported that *Trp53* $^{-/-}$ mice had an opposite phenotype, characterized by the presence of increased neuroblasts (Gil-Perotin *et al.*, 2006). Consistent with the opposite phenotype of *Trp53* $^{-/-}$ and *p27* $^{Kip1-/-}$ mice, double mutant *Trp53* $^{-/-}$*;p27* $^{Kip1-/-}$ mice had a number of neuroblasts equivalent to wild-type mice. The opposing effect of loss of *Trp53* or *Cdknb1* on neurogenesis is supported by considerable evidence, including immunohistochemical, ultrastructural and behavioral data. It is worth mentioning that aSVZ newly born neuroblasts have been shown to migrate to the OB, where they integrate into pre-existing neural networks and play a critical role in odor habituation (Magavi *et al.*, 2005), a form of olfactory memory elicited after exposure to novel odors. When blindly assessed for exploratory time of novel and habituated odors, mice of the four distinct genotypes showed significant differences in behavior that correlated with the number of adult born neuroblasts.

The *Trp53* $^{-/-}$ mice showed a trend of spending more time on the novel odor compared with habituated or familiar odors, in agreement with a greater number of newly born neurons in the OB. In contrast, the *p27* $^{Kip1-/-}$ mice spent a similar amount of time exploring the novel and the habituated odor, as if unable to acknowledge the fact that the odor had been previously presented. Furthermore, this group showed clear memory impairment and a reduced number of newly born neuroblasts in the OB.

This defective memory was partially restored in the *Trp53* $^{-/-}$ *p27* $^{Kip1-/-}$ double mutant mice, which were also characterized by a similar number of newly born neuroblasts to wild-type. Together, these data suggest that p53 and p27 ^{Kip1} might have opposing roles in adult neurogenesis and this could explain the partial complementation of the novel odor-seeking behavioral phenotype, detected in the double knockout mice.

Cellular and molecular mechanisms underlying the effect of p53 and p27 ^{Kip1} in modulating adult neurogenesis

One of the simplest explanations of the compensatory effect on neuroblast number in the SVZ of *Trp53* $^{-/-}$*;p27* $^{Kip1-/-}$ mice compared with *Trp53* $^{-/-}$ or *p27* $^{Kip1-/-}$ mice was survival. This interpretation was supported by the detection of fewer apoptotic cells in the SVZ of *Trp53* $^{-/-}$*;p27* $^{Kip1-/-}$ mice compared with *p27* $^{Kip1-/-}$ mice. However, the *in vitro* data in cultured SVZ cells and studies in embryonic neural precursors lacking *Trp53* (Armesilla-Diaz *et al.*, 2009) or *p27* ^{Kip1} (Nguyen *et al.*, 2006) suggested the possibility that *p53* and *p27* ^{Kip1} might also directly modulate the transcriptional effectors of the neurogenic program, independent of survival.

For p27 ^{Kip1} it was previously reported that it modulates neurogenesis in the developing brain by binding with its N terminus to the neurogenic transcription factor Ngn2 and regulating its stability by protecting it from ubiquitination (Nguyen *et al.*, 2006). However, immunohistochemical studies in the neonatal SVZ (Roybon *et al.*, 2009) and genetic fate-mapping studies in the adult brain, using mice genetically engineered to express the reporter green fluorescent protein from the endogenous *Ngn2* locus (Brill *et al.*, 2009), suggested a much more restricted expression of Ngn2 to specific subpopulations of neurons. Our study suggests an interaction between p27 ^{Kip1} and the transcription factor Ngn2 also in protein extracts from the aSVZ and OB. This interaction was identified using a co-

immunoprecipitation approach of protein lysates and different antibodies specific for the N-terminal region of the murine Ngn2. It is important to mention that we obtained successful co-immunoprecipitation only when we used affinity-purified antibodies that were raised against the amino acids 86–98 of mouse Ngn2, while other studies reporting immunocytochemical identification of Ngn2 cells used a goat antibody raised against human Ngn2. When we conducted a sequence homology analysis between human and murine Ngn2, we noted that the highest level of homology occurs in the central region of the molecule, which corresponds to the basic Helix-Loop_helix transcription factor and DNA-binding motif. Therefore, the antibodies used in our immunoprecipitation studies were directed towards the N terminus of the murine Ngn2, which is also the least conserved region between the two species. In addition, it is important to mention here that the co-immunoprecipitation technique would have enriched the detection of the two interacting molecules, as the studies required at least 1–2 mg of protein lysates prepared from several pooled tissues. Thus, we believe that the differences between our results and those obtained by other studies (Brill *et al.*, 2009; Roybon *et al.*, 2009) are not contradictory but rather reflect the different use of distinct techniques and reagents. Additional evidence to support the functional relevance of the interaction between Ngn2 and p27 ^{Kip1} was provided by the results in cells cultured from wild-type and *p27* $^{Kip1-/-}$ mice. It had been proposed that in the embryonic brain, the interaction with p27 ^{Kip1} protects Ngn2 from proteasomal degradation (Nguyen *et al.*, 2006). As we detected a similar interaction in the adult SVZ, we reasoned that we could rescue the low numbers of neuroblasts in *p27* $^{Kip1-/-}$ cultures by incubating them in the presence of the proteasome inhibitor MG132. Indeed, *p27* $^{Kip1-/-}$ SVZ cultures treated with MG132 had a similar number of neuroblasts to wild-type SVZ cultures during the first 3 days in differentiation conditions. It is worth noting that the effect of the proteasomal inhibitor was more evident at the early time points and is consistent with the stabilization of neurogenic factors that are needed during the early stages of the neurogenic program of transcription.

The evidence that p53 function negatively affects neurogenesis is consistent with the results of a large number of studies, including our previous reports in the adult SVZ (Gil-Perotin *et al.*, 2006). It was previously reported that suppression of p53 activity in fetal cerebellar neurons accelerates their terminal differentiation (Ferreira & Kosik, 1996) and in neurospheres from fetal OB favors neuronal differentiation (Armesilla-Diaz *et al.*, 2009). It is also consistent with the phenotype of transgenic mice expressing a truncated but transcriptionally active form of p53, which are characterized by a reduced number of neural stem cells in the SVZ and reduced neurons in the OB (Medrano *et al.*, 2009). Because loss of *Trp53* rescued the decreased neurogenic phenotype observed in *p27* $^{Kip1-/-}$ mice and p27 ^{Kip1} affected protein stability of neurogenic transcription factors, in this study we asked whether additional neurogenic molecules could be affected by p53. We detected precocious expression of *NeuroD* and *Math3* in cultured *Trp53* $^{-/-}$ cells, a finding that is consistent with previous reports in a clonal astrocyte progenitor cell line derived from p53-deficient fetal brains (Horiuchi & Tomooka, 2005), and that resulted in a precocious generation of TuJ1-positive cells. Thus, we suggest that p53 and p27 ^{Kip1} differentially modulate neurogenesis by regulating the neurogenic transcriptional network (Fig. 8). However, we cannot exclude the possibility that additional pathways are modulated by p53, as a recent report has suggested the potential involvement of the Notch pathway (Roybon *et al.*, 2009). Overall it is highly likely that global knockout of transcriptional regulators might affect neurogenesis cell-autonomously by modulating the neurogenic transcriptional network, and non-autonomously by modulating the availability of extrinsic factors.

In conclusion, we have identified p53 and p27 ^{Kip1} as two important regulators of aSVZ cell proliferation and adult neurogenesis.

Acknowledgments

We thank Mr L. Franco and Ms C. Capillini for help with some experiments. This work was supported by grants RO1 NS52738 and RG-4134 from the National Multiple Sclerosis Society to P.C., CA096832 to M.F.R. J.D.H. holds a postdoctoral fellowship from the Multiple Sclerosis Society of Canada and the Fonds de la recherche en santé du Québec.

Abbreviations

ANOVA	analysis of variance
aNSCs	adult neural stem cells
aSVZ	adult subventricular zone
GFAP	glial fibrillary acidic protein
Ngn2	Neurogenin 2
OB	olfactory bulb
RMS	rostral migratory stream
SVZ	subventricular zone

References

Andela VB, Rosier RN. The proteosome inhibitor MG132 attenuates retinoic acid receptor trans-activation and enhances trans-repression of nuclear factor kappaB. Potential relevance to chemo-preventive interventions with retinoids. Mol Cancer. 2004; 3:8. [PubMed: 15035668]

Armesilla-Diaz A, Bragado P, Del Valle I, Cuevas E, Lazaro I, Martin C, Cigudosa JC, Silva A. p53 regulates the self-renewal and differentiation of neural precursors. Neuroscience. 2009; 158:1378–1389. [PubMed: 19038313]

Brill MS, Ninkovic J, Winpenny E, Hodge RD, Ozen I, Yang R, Lepier A, Gascon S, Erdelyi F, Szabo G, Parras C, Guillemot F, Frotscher M, Berninger B, Hevner RF, Raineteau O, Gotz M. Adult generation of glutamatergic olfactory bulb interneurons. Nat Neurosci. 2009; 12:1524–1533. [PubMed: 19881504]

Doetsch F. A niche for adult neural stem cells. Curr Opin Genet Dev. 2003; 13:543–550. [PubMed: 14550422]

Doetsch F, Garcia-Verdugo JM, Alvarez-Buylla A. Cellular composition and three-dimensional organization of the subventricular germinal zone in the adult mammalian brain. J Neurosci. 1997; 17:5046–5061. [PubMed: 9185542]

Doetsch F, Caille I, Lim DA, Garcia-Verdugo JM, Alvarez-Buylla A. Subventricular zone astrocytes are neural stem cells in the adult mammalian brain. Cell. 1999; 97:703–716. [PubMed: 10380923]

Doetsch F, Verdugo JM, Caille I, Alvarez-Buylla A, Chao MV, Casaccia-Bonnefil P. Lack of the cell-cycle inhibitor p27Kip1 results in selective increase of transit-amplifying cells for adult neurogenesis. J Neurosci. 2002; 22:2255–2264. [PubMed: 11896165]

Fero ML, Rivkin M, Tasch M, Porter P, Carow CE, Firpo E, Polyak K, Tsai LH, Broudy V, Perlmutter RM, Kaushansky K, Roberts JM. A syndrome of multiorgan hyperplasia with features of gigantism, tumorigenesis, and female sterility in p27(Kip1)-deficient mice. Cell. 1996; 85:733–744. [PubMed: 8646781]

Ferreira A, Kosik KS. Accelerated neuronal differentiation induced by p53 suppression. J Cell Sci. 1996; 109:1509–1516. [PubMed: 8799837]

Gil-Perotin S, Marin-Husstege M, Li J, Soriano-Navarro M, Zindy F, Roussel MF, Garcia-Verdugo JM, Casaccia-Bonnefil P. Loss of p53 induces changes in the behavior of subventricular zone cells: implication for the genesis of glial tumors. J Neurosci. 2006; 26:1107–1116. [PubMed: 16436596]

He Y, Dupree J, Wang J, Sandoval J, Li J, Liu H, Shi Y, Nave KA, Casaccia-Bonnefil P. The transcription factor Yin Yang 1 is essential for oligodendrocyte progenitor differentiation. Neuron. 2007; 55:217–230. [PubMed: 17640524]

Horiuchi M, Tomooka Y. An attempt to generate neurons from an astrocyte progenitor cell line FBD-104. Neurosci Res. 2005; 53:104–115. [PubMed: 16054258]

Johansson CB, Svensson M, Wallstedt L, Janson AM, Frisen J. Neural stem cells in the adult human brain. Exp Cell Res. 1999; 253:733–736. [PubMed: 10585297]

Kiyokawa H, Koff A. Roles of cyclin-dependent kinase inhibitors: lessons from knockout mice. Curr Top Microbiol Immunol. 1998; 227:105–120. [PubMed: 9479827]

Lamolet B, Poulin G, Chu K, Guilemot F, Tsai MJ, Drouin J. Tpit-independent function of NeuroD1(BETA2) in pituitary corticotroph differentiation. Mol Endocrinol. 2004; 18:995–1003. [PubMed: 14726486]

Li J, Ghiani CA, Kim JY, Liu A, Sandoval J, DeVellis J, Casaccia-Bonnefil P. Inhibition of p53 transcriptional activity: a potential target for future development of therapeutic strategies for primary demyelination. J Neurosci. 2008; 28:6118–6127. [PubMed: 18550754]

Lois C, Alvarez-Buylla A. Proliferating subventricular zone cells in the adult mammalian forebrain can differentiate into neurons and glia. Proc Natl Acad Sci USA. 1993; 90:2074–2077. [PubMed: 8446631]

Lois C, Garcia-Verdugo JM, Alvarez-Buylla A. Chain migration of neuronal precursors. Science. 1996; 271:978–981. [PubMed: 8584933]

Ma YC, Song MR, Park JP, Henry Ho HY, Hu L, Kurtev MV, Zieg J, Ma Q, Pfaff SL, Greenberg ME. Regulation of motor neuron specification by phosphorylation of neurogenin 2. Neuron. 2008; 58:65–77. [PubMed: 18400164]

Magavi SS, Mitchell BD, Szentirmai O, Carter BS, Macklis JD. Adult-born and preexisting olfactory granule neurons undergo distinct experience-dependent modifications of their olfactory responses in vivo. J Neurosci. 2005; 25:10729–10739. [PubMed: 16291946]

McAllister SS, Becker-Hapak M, Pintucci G, Pagano M, Dowdy SF. Novel p27(kip1) C-terminal scatter domain mediates Rac-dependent cell migration independent of cell cycle arrest functions. Mol Cell Biol. 2003:23.

Medrano S, Burns-Cusato M, Atienza MB, Rahimi D, Scrable H. Regenerative capacity of neural precursors in the adult mammalian brain is under the control of p53. Neurobiol Aging. 2009; 30:483–497. [PubMed: 17850928]

Menn B, Garcia-Verdugo JM, Yaschine C, Gonzalez-Perez O, Rowitch D, Alvarez-Buylla A. Origin of oligodendrocytes in the subventricular zone of the adult brain. J Neurosci. 2006; 26:7907–7918. [PubMed: 16870736]

van Meyel DJ, Ramsay DA, Casson AG, Keeney M, Chambers AF, Cairncross JG. p53 mutation, expression, and DNA ploidy in evolving gliomas: evidence for two pathways of progression. J Natl Cancer Inst. 1994; 86:1011–1017. [PubMed: 8007011]

Mirzadeh Z, Merkle FT, Soriano-Navarro M, Garcia-Verdugo JM, Alvarez-Buylla A. Neural stem cells confer unique pinwheel architecture to the ventricular surface in neurogenic regions of the adult brain. Cell Stem Cell. 2008; 3:265–278. [PubMed: 18786414]

Monaghan MM, Leddy L, Sung ML, Albinson K, Kubek K, Pangalos MN, Reinhart PH, Zaleska MM, Comery TA. Social odor recognition: a novel behavioral model for cognitive dysfunction in Parkinson's disease. Neurodegen Dis. 2010; 7:153–159.

Morrison SJ, Shah NM, Anderson DJ. Regulatory mechanisms in stem cell biology. Cell. 1997; 88:287–298. [PubMed: 9039255]

Mullen RJ, Buck CR, Smith AM. NeuN, a neuronal specific nuclear protein in vertebrates. Development. 1992; 116:201–211. [PubMed: 1483388]

Nguyen L, Besson A, Heng JI, Schuurmans C, Teboul L, Parras C, Philpott A, Roberts JM, Guillemot F. p27kip1 independently promotes neuronal differentiation and migration in the cerebral cortex. Genes Dev. 2006; 20:1511–1524. [PubMed: 16705040]

O'Dell SJ, Feinberg LM, Marshall JF. A neurotoxic regimen of methamphetamine impairs novelty recognition as measured by a social odor-based task. Behav Brain Res. 2010; 216:396–401. [PubMed: 20797410]

Park KH, Lee J, Yoo CG, Kim YW, Han SK, Shim YS, Kim SK, Wang KC, Cho BK, Lee CT. Application of p27 gene therapy for human malignant glioma potentiated by using mutant p27. J Neurosurg. 2004; 101:505–510. [PubMed: 15352609]

Picard-Riera N, Nait-Oumesmar B, Baron-Van Evercooren A. Endogenous adult neural stem cells: limits and potential to repair the injured central nervous system. J Neurosci Res. 2004; 76:223–231. [PubMed: 15048920]

Rane NS, Yonkovich JL, Hegde RS. Protection from cytosolic prion protein toxicity by modulation of protein translocation. EMBO J. 2004; 23:4550–4559. [PubMed: 15526034]

Rasheed BK, McLendon RE, Herndon JE, Friedman HS, Friedman AH, Bigner DD, Bigner SH. Alterations of the TP53 gene in human gliomas. Cancer Res. 1994; 54:1324–1330. [PubMed: 8118823]

Recht L, Jang T, Savarese T, Litofsky NS. Neural stem cells and neuro-oncology: quo vadis? J Cell Biochem. 2003; 88:11–19. [PubMed: 12461769]

Reynolds BA, Tetzlaff W, Weiss S. A multipotent EGF-responsive striatal embryonic progenitor cell produces neurons and astrocytes. J Neurosci. 1992; 12:4565–4574. [PubMed: 1432110]

Roybon L, Deierborg T, Brundin P, Li JY. Involvement of Ngn2, Tbr and NeuroD proteins during postnatal olfactory bulb neurogenesis. Eur J Neurosci. 2009; 29:232–243. [PubMed: 19200230]

Seri B, Garcia-Verdugo JM, Collado-Morente L, McEwen BS, Alvarez-Buylla A. Cell types, lineage, and architecture of the germinal zone in the adult dentate gyrus. J Comp Neurol. 2004; 478:359–378. [PubMed: 15384070]

Sherr CJ, Roberts JM. Inhibitors of mammalian G1 cyclin-dependent kinases. Genes Dev. 1995; 9:1149–1163. [PubMed: 7758941]

Spinetta MJ, Woodlee MT, Feinberg LM, Stroud C, Schallert K, Cormack LK, Schallert T. Alcohol-induced retrograde memory impairment in rats: prevention by caffeine. Psychopharmacology (Berl). 2008; 201:361–371. [PubMed: 18758756]

Sun F, Anantharam V, Zhang D, Latchoumycandane C, Kanthasamy A, Kanthasamy AG. Proteasome inhibitor MG-132 induces dopaminergic degeneration in cell culture and animal models. Neurotoxicology. 2006; 27:807–815. [PubMed: 16870259]

Temme A, Geiger KD, Wiedemuth R, Conseur K, Pietsch T, Felsberg J, Reifenberger G, Tatsuka M, Hagel C, Westphal M, Berger H, Simon M, Weller M, Schackert G. Giant cell glioblastoma is associated with altered aurora b expression and concomitant p53 mutation. J Neuropathol Exp Neurol. 2010; 69:632–642. [PubMed: 20467329]

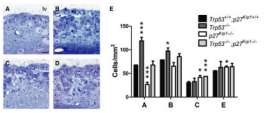

Fig. 1.

Functional antagonism between p27^{Kip1} and p53 in regulating the number of neuroblasts in the adult SVZ. (A–D) Semithin sections of the SVZ of wild-type (A), *Trp53*$^{-/-}$ (B), *p27* $^{Kip1-/-}$ (C) and *Trp53*$^{-/-}$;*p27* $^{Kip1-/-}$ (D) mice stained with toluidine blue. Note the difference in thickness of the cellular layer in *Trp53*$^{-/-}$ (B) and in *Trp53*$^{-/-}$;*p27* $^{Kip1-/-}$ (D) mice compared with wild-type (A) and *p27* $^{Kip1-/-}$ (C). Scale bar = 25 μm; lv, lateral ventricle. (E) Bar graph of the average number of SVZ cells identified in the SVZ of mice of the indicated genotypes per unit length (wild-type $n = 5$, *Trp53*$^{-/-}$ $n = 5$, *p27* $^{Kip1-/-}$ $n = 4$, *Trp53*$^{-/-}$;*p27* $^{Kip1-/-}$ $n = 4$) $^{*}P < 0.05$, $^{***}P < 0.001$, compared with wild-type for each cell type, using one-way ANOVA followed by Dunnett's multiple-comparison test.

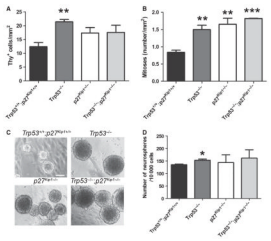

Fig. 2.

The cell cycle regulators p53 and $p27^{Kip1}$ both act as negative regulators of cell cycle entry in the adult SVZ *in vivo*. (A) Quantification of the total number of cells labeled in the SVZ of mice of the indicated genotype, after a fast pulse of ^{3}[H]-thymidine incorporation. (B) Quantification of the number of mitoses detected by electron microscopy and referred by surface area. (C) Bright-field appearance of primary neurospheres cultured from the SVZ of the mice of indicated genotype. Scale bar = 200 μm. (D) Number of primary neurospheres formed after plating freshly dissected SVZ cells at a density of 10 000 cells/mL. *$P < 0.05$, **$P < 0.01$, ***$P < 0.001$ compared with wild-type for each cell type.

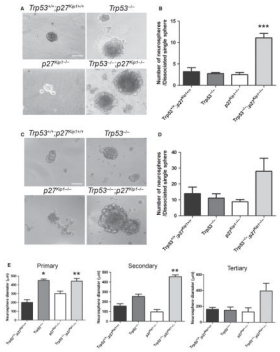

Fig. 3.

Effect of genetic deletion of *Trp53* and/or *p27 Kip1* in regulating clonogenic ability of cultured aSVZ cells. (A) Bright-field images of representative fields of secondary neurospheres generated from dissociation of single neurospheres into cell suspension. Scale bar = 200 μm. (B) Quantification of secondary neurospheres generated after dissociation of single neurospheres. (C) Bright-field images of representative fields of tertiary neurospheres generated from dissociation of single neurospheres into cell suspension and replating in low attachment plates. Scale bar = 200 μm. (D) Quantification of tertiary spheres generated from dissociation of individual spheres. (E) Quantification of the neurosphere size in primary, secondary and tertiary passages. *P < 0.05, **P < 0.01, ***P < 0.001, compared with wild-type for each cell type, using t-test.

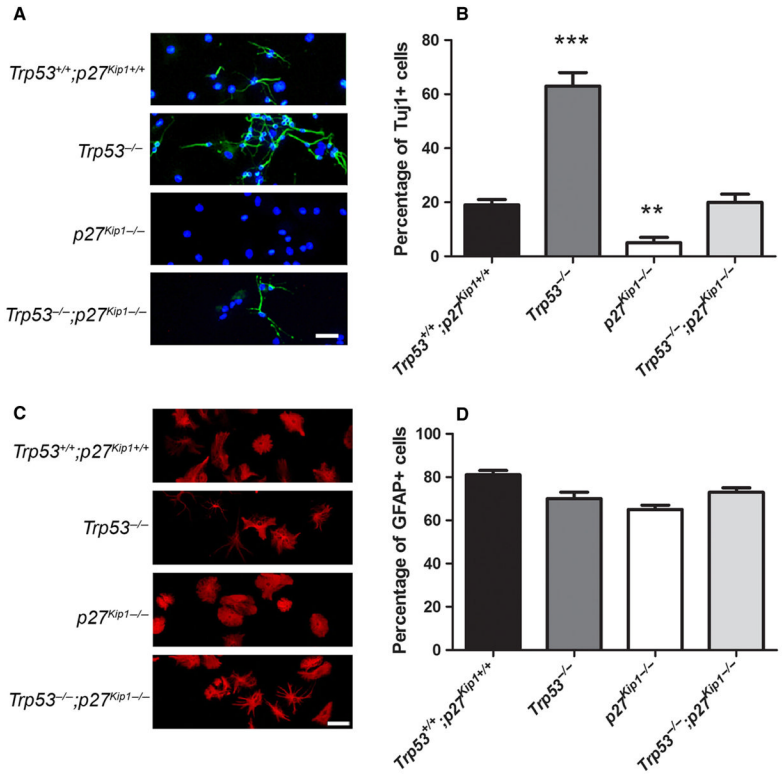

Fig. 4.

Antagonistic roles of p53 and $p27^{Kip1}$ in adult neurogenesis, but not gliogenesis *in vitro*. (A) *In vitro* differentiation of neurospheres generated from animals of the indicated genotype. After dissociation and replating in chemically defined medium for 7 days, cultures were stained with antibodies for TuJ1 (green) to identify neuroblasts and with DAPI (blue) to counterstain nuclei. Scale bar = 50 μm. (B) Bar graphs indicating the number of TuJ1+ cells relative to DAPI+ nuclei. Note the increased number of TuJ1+ cells in $Trp53^{-/-}$ and the lower number in $p27^{Kip1-/-}$ mutants compared with the other genotypes, as previously described. (C) Confocal image of aSVZ cultured cells isolated from mice of the indicated genotype, stained with antibodies for GFAP (red), as a marker for astrocytes and stem-like cells. Note the presence of astrocytes with altered protoplasmic morphology in the $Trp53^{-/-}$ and $Trp53^{-/-};p27^{Kip1-/-}$ animals compared with the other genotypes. Scale bar = 50 μm. (D) Bar graphs indicating the number of GFAP+ cells relative to the number of DAPI+ nuclei. There was no significant difference in the number of GFAP+ cells among the distinct genotypes. Statistical differences for B and D were determined using the Mann–Whitney *U*-test (**$P < 0.01$, ***$P < 0.001$). For interpretation of color references in figure legend, please refer to the Web version of this article.

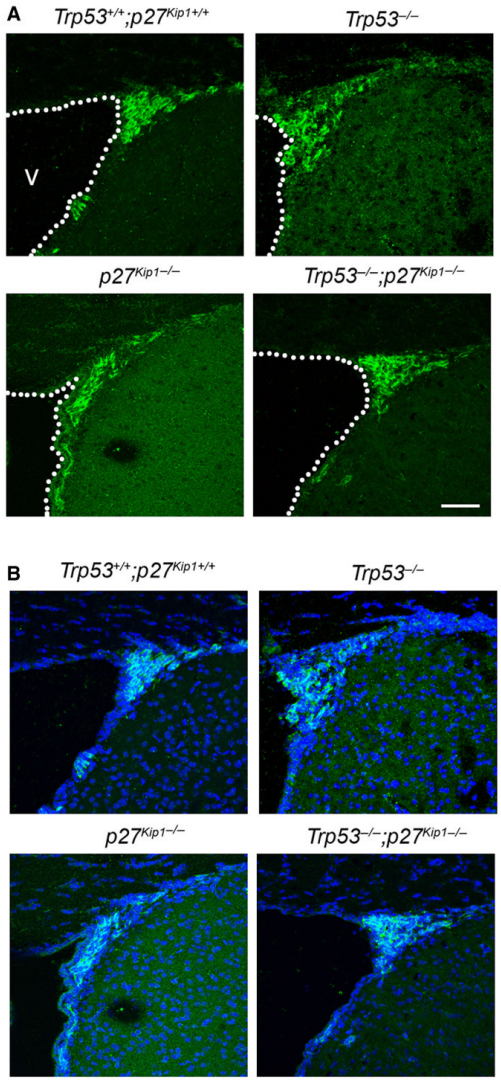

Fig. 5.

Genetic deletion of *Trp53* and *p27 Kip1* has opposing effects on neurogenesis *in vivo*. Confocal image of the adult SVZ (dashed line) from mice of the indicated genotype, stained with antibodies for doublecortin (green in B) as markers for newly formed neuroblasts. DAPI (blue) was used as nuclear counterstain (merge, B). Scale bar = 50 μm. v, lateral ventricle. For interpretation of color references in figure legend, please refer to the Web version of this article.

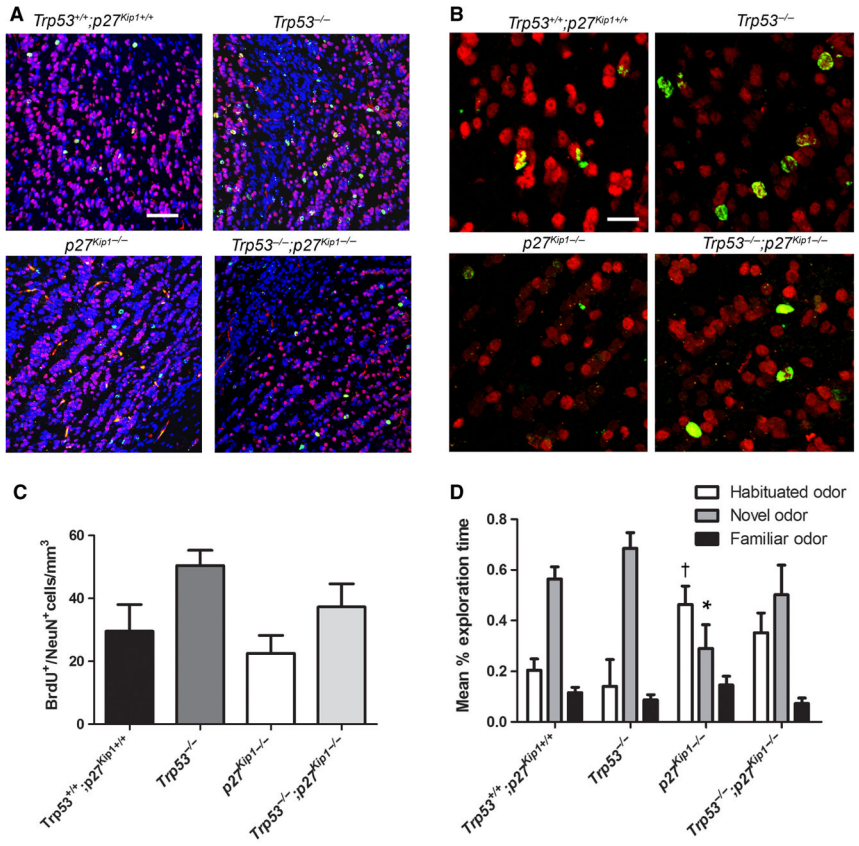

Fig. 6.

Differences in odor recognition behavior in mice with genetic deletion of *Trp53*, *p27 Kip1* or both correlate with the number of adult neuroblasts in the OB. (A) Representative low-magnification confocal microscopy images depicting the BrdU+ (green)/NeuN+ (red) cells incorporated in the OB of the four distinct genotypes (nuclear staining DAPI, blue). Scale bar = 30 μm. (B) High-magnification images of the figures shown in A, showing only the double positive BrdU+ (green)/NeuN+ (red) cells. Scale bar = 10 μm. (C) Bar graph of the number of newly generated neuroblasts per volume unit (cell number/mm^3) for each genotype. (D) Time of exploratory behavior towards habituated odors, novel odors and familiar odors measured in mice of the indicated genotype. †Statistical significance of the exploratory behavior towards the habituated odor ($P < 0.05$); *statistically significant decreased time spent exploring the novel odor ($P < 0.05$) by the *p27 Kip1 −/−* mice compared with wild-type. For interpretation of color references in figure legend, please refer to the Web version of this article.

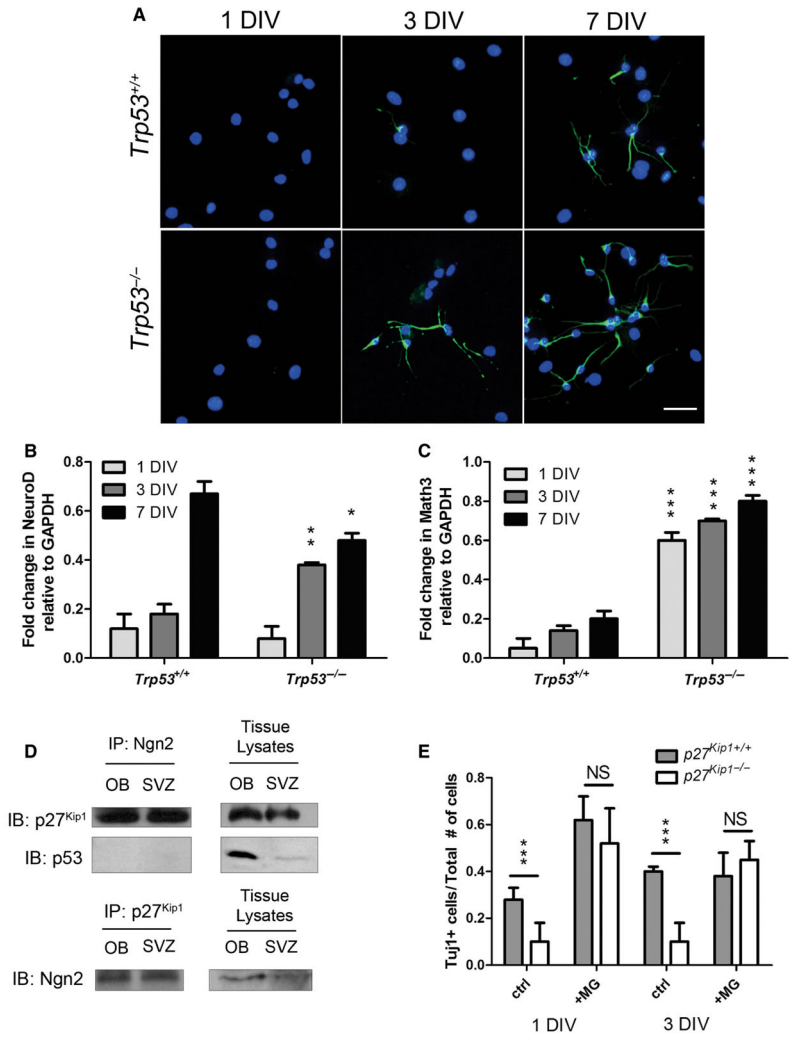

Fig. 7.

Enhanced neurogenesis of *Trp53*$^{-/-}$ neurospheres by induction of neuronal basic Helix-Loop_helix transcription factor genes. p27^{Kip1} binds neurogenin and promotes its stability to regulate neurogenesis. (A) Time-course of *in vitro* neurogenesis of SVZ-derived precursors isolated from wild-type and *Trp53*$^{-/-}$ mutants 1, 3 and 7 days *in vitro* (DIV) after dissociation and plating in chemically defined medium. Note the higher level of neuroblasts detected in *Trp53*$^{-/-}$ cells at the 3-day time point. Scale bar = 50 μm. (B and C) qPCR of *NeuroD* (B) and *Math3* (C) transcript levels in RNA samples isolated from wild-type and *Trp53*$^{-/-}$ dissociated neurospheres after 1, 3 or 7 days in differentiation conditions (DIV1, DIV3 and DIV7). The higher transcript levels detected in the *Trp53*$^{-/-}$ mutants compared with wild-type were statistically significant (***$P < 0.001$, independent two-tailed *t*-test). (D) Immunoprecipitation of protein extracts from the OB and the SVZ of wild-type mice, using antibodies against Ngn2 or p27^{Kip1} and immunoblotting with antibodies specific for p27^{Kip1}, Ngn2 and p53 proteins. (E) TuJ1-positive cells derived from *p27* $^{Kip1-/-}$ mice after differentiation in chemically define medium without mitogens for 1 or 3 DIV in the absence (ctrl) or presence of 5 μM MG132. *$P < 0.05$, **$P < 0.01$, ***$P < 0.001$ (*t*-test).

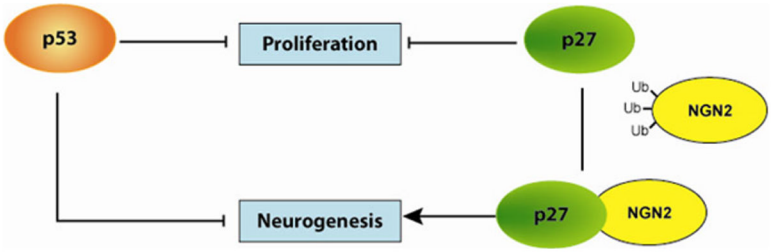

Fig. 8.

Model of the functional interaction between p53 and $p27^{Kip1}$ in modulating the behavior of adult SVZ cells. We propose a model that includes a similar although not synergistic interaction between two cell cycle regulators in modulating proliferation and an opposing role in the regulation of neurogenesis. For p53 the negative regulation of neurogenesis may be mediated by transcriptional and non-transcriptional targets, while for $p27^{Kip1}$, the positive effect on neurogenesis is dependent on the increased stability of Ngn2.

Table 1

Antibodies used in this study

Antibody	Host	Antigen	Dilution	Company, cat. no.	Specificity
*β*III-tubulin (TuJ1)	Monoclonal mouse	Microtubules from rat brain	1: 500 (ICC)	Covance (Richmond, CA, USA), MMS-435P	Young neurons (Doetsch *et al.*, 1997)
BrdU	Monoclonal mouse	BSA-conjugated BrdU	1: 200 (IHC)	Dako, M0744	S-phase exogenous marker
BrdU	Monoclonal rat	BSA-conjugated BrdU	1: 150 (IHC)	Abcam (Cambridge, UK), AB6326	S-phase exogenous marker
NeuN (clone A60)	Monoclonal mouse	Purified nuclei from mouse brain	1: 500 (IHC)	Chemicon Millipore, MAB377	Most neuronal cell types Positive control: brain tissue (Mullen *et al.*, 1992)
Ngn2	Rabbit polyclonal IgG	Synthetic peptide, amino acids 85–97 of mouse Ngn2	1: 500 (WB)	Millipore, AB55682	(Lamolet *et al.*, 2004)
Ngn2	Rabbit polyclonal IgG	BSA conjugated to amino acids 85–97 of mouse Ngn2	10 *μ*g (IP)	Sigma-Aldrich, N6286	
Ngn2	Rabbit IgG	Mouse Ngn2	1: 200 (WB)	Y.-C. Ma, gift	(Ma *et al.*, 2008)
$p27^{Kip1}$ (C-19)	Polyclonal rabbit IgG	Peptide at the C terminus of human p27	10 *μ*g (IP)	Santa Cruz, sc-528	Antibody specificity validated using $p27^{Kip1-/-}$ mouse brain lysates Purified recombinant p27 protein used as positive control (Santa Cruz, sc-4091)
$p27^{Kip1}$ (C-19)-HRP conjugated antibody	Polyclonal rabbit IgG	Peptide at the C terminus of human p27	1: 500 (WB)	Santa Cruz, sc-528 HRP	
GFAP, Clone 6F2	Mouse monoclonal Isotype IgG1, kappa	GFAP from human brain	1: 250	Dako, M076101	Astrocytes